Tetrahedron 67 (2011) 6889–6894

Contents lists available at ScienceDirect

Tetrahedron

journal homepage: www.elsevier.com/locate/tet

Radical intermediates in the photorearrangement of 3-hydroxyindolic nitrones

Angelo Alberti [a], Paola Astolfi [b], Patricia Carloni [b], Dietrich Döpp [c], Lucedio Greci [b,*], Corrado Rizzoli [d], Pierluigi Stipa [b]

[a] ISOF-CNR, Area della Ricerca di Bologna, Via P. Gobetti 101, I-40129 Bologna, Italy
[b] Dipartimento ISAC-Sezione Chimica, Università Politecnica delle Marche, Via Brecce Bianche, I-60131 Ancona, Italy
[c] Fachgebiet Organische Chemie, Universität Duisburg-Essen, D-45117 Essen, Germany
[d] Dipartimentio di Chimica Generale, Chimica Analitica e Chimica Fisica, Università di Parma, Viale delle Scienze 17/4, I-43100 Parma, Italy

ARTICLE INFO

Article history:
Received 7 March 2011
Received in revised form 9 June 2011
Accepted 24 June 2011
Available online 30 June 2011

Keywords:
Nitrone photochemistry
Oxaziridine intermediates
DFT calculations
EPR spectroscopy
Spin trapping

ABSTRACT

A number of 3-hydroxy substituted indolic nitrones were found to quantitatively photorearrange to (2-benzoylamino)phenyl ketones upon UV-A irradiation. EPR-Spin Trapping experiments suggest that the process, which is believed to proceed via the formation of an oxaziridine, follows a homolytic pathway. Although DFT calculations do not allow to totally exclude alternative routes involving singlet intermediates, they do provide support to the proposed homolytic mechanism, which would be driven by a 1,5-hydrogen transfer subsequent to the oxaziridine ring opening. When this hydrogen transfer was made impossible by methylation of the 3-OH group, a benzoxazine was isolated as the sole reaction product.

1. Introduction

The photochemistry of nitrones and *N*-oxides has been extensively studied and since the '70s a number of papers and reviews on this topic have appeared.[1–10] In most cases, the reaction is described to proceed through the intermediate formation of an oxaziridine derivative, which can be isolated or, being itself photochemically reactive, rearranges to an amide, lactam, benzoxazine, etc. Different ionic, radical or concerted mechanisms have been proposed for the subsequent transformation of the oxaziridine,[6,11,12] but in very few occasions the involvement of a particular intermediate has been evidenced. For example, the rearrangement of 2-phenylisatogen to 2-phenyl-4*H*-3,1-benzoxazin-4-one is described to proceed via a biradical intermediate,[4] as a precursor of a ketene, but without any experimental evidence. Similar results are reported for 2-phenyl-3-arylimino-3*H*-indole *N*-oxides.[13] Trapping experiments using 2,3-dimethylbut-2-ene or other less substituted alkenes or dienes supported the involvement of a biradical in the photochemistry of phenanthridine *N*-oxides,[5,7] although only in particular cases and according to the nature of the solvent and of the substituents on the α-carbon.

We report here on the photo-induced rearrangement of 2-phenyl-3-hydroxy-3-alkyl/aryl-indoline-*N*-oxides **1a**–**f** to alkyl/aryl-(2-benzoylamino)phenyl ketones **2a**–**f** (see Scheme 1) in almost quantitative yield and propose a radical-based mechanism for the process. When the reactions were carried out inside the cavity of an Electron Paramagnetic Resonance (EPR) spectrometer in the presence of the spin-trap PBN (*N*-*tert*-butyl-α-phenyl-nitrone), radical intermediates were trapped in the form of nitroxidic spin-adducts in agreement with the suggested mechanism, which was also supported by the results of Density Functional Theory (DFT) calculations.

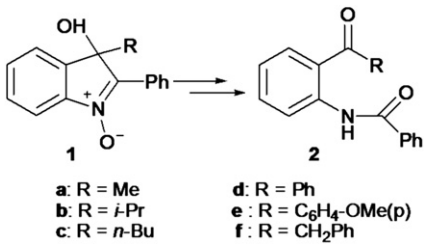

Scheme 1.

* Corresponding author. Tel.: +39 071 2204408; fax: +39 071 2204714; e-mail address: l.greci@univpm.it (L. Greci).

0040-4020/$ – see front matter © 2011 Elsevier Ltd. All rights reserved.
doi:10.1016/j.tet.2011.06.094

2. Results and discussion

When acetonitrile solutions of compounds **1a**–**f** were irradiated with a UV-A lamp in a quartz tube for 20 min under stirring, the sole products obtained in the reactions were the amidic derivatives **2a**–**f** (Scheme 1), identified on the basis of their IR and ^{1}H NMR spectral data. In particular, all products **2a**–**f** showed in their IR spectra a broad band at ca. 3200 cm^{-1} and absorptions at ca. 1675 cm^{-1} and 1580 cm^{-1}, corresponding to the ketonic and amidic carbonyl groups, respectively. Moreover, the structure of compound **2d** was unambiguously determined by X-ray diffractometry as shown in Fig. 1. Bond lengths and angles are not unusual and in good agreement with those observed in the strictly related compound 4-acetyl-2,*N*-dibenzoylaniline.[14] In compound **2d**, the amidic and ketonic carbonyl groups are slightly twisted with respect to the central benzene ring, as indicated, also in the molecular geometry computed 'in vacuo' at the B3-LYP/6-31G(d) level (values in parenthesis), by the angles of 4.60° (2.74) and 10.55° (23.30) formed by the C8–C13 benzene ring with the mean planes of the C7/O1/N1/C8 and C13/C14/C15/O2 groups, respectively. The angles between the C8–C13 benzene ring with the C1–C6 and C15–C20 phenyl rings are 15.31° (12.32) and 61.88° (64.36), respectively. In addition, the molecular conformation is stabilized by an intramolecular N–H·O hydrogen bond forming a six-membered ring: N1–H1, 0.86 Å (1.02); H1·O2, 1.92 Å (1.80); N1·O2, 2.63 Å (2.66); N1–H1·O2, 139° (139). The crystal packing, likely responsible of the slight differences between experimental and computed geometries, is governed only by Van der Waals interactions.

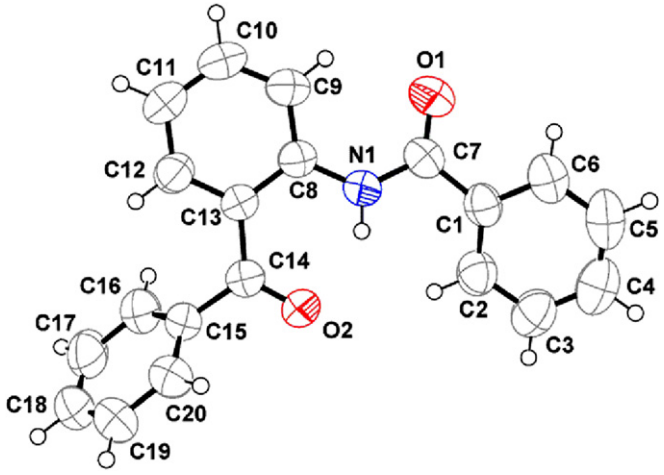

Fig. 1. Molecular structure of **2d**, with displacement ellipsoids drawn at the 50% probability level.

Photorearrangement of nitrones and *N*-oxides is commonly described to proceed with formation of oxaziridines, whose three-membered rings are in many cases rather unstable and easily react further following different reaction pathways. In particular, the initially formed oxaziridines, which are photo- and thermolabile, generally rearrange to amides.[3] This is what happens also in the reactions described in the present work: compounds **2a**–**f** obtained upon UV-irradiation of the studied nitrones could actually derive from an oxaziridine intermediate **3** through a radical path (Scheme 2). In fact, the homolytic cleavage of the N–O bond in the oxaziridine ring could lead to an alkoxy-aminyl biradical **4** and, upon cleavage of the C_α-C_β bond, to the biradical **5**/**5**′, that may exist either in a singlet or in a triplet state. An H-transfer in **5**′ accounts for the eventual formation of the isolated compound **2**. Although in most cases photorearrangement of nitrones via oxaziridine intermediates is described as a reaction leading to a fairly complex products distribution, noteworthily we obtained products **2** in more than 90% yield in all the reactions performed, without the significant formation of any side products. For example, from the irradiation of 2-unsubstituted 3*H*-indole *N*-oxides,[15–17] several products were isolated derived from ring enlargement to form a benzoxazine derivative, ring opening and H-shift to generate an isocyanate, and isomerization to a lactam.

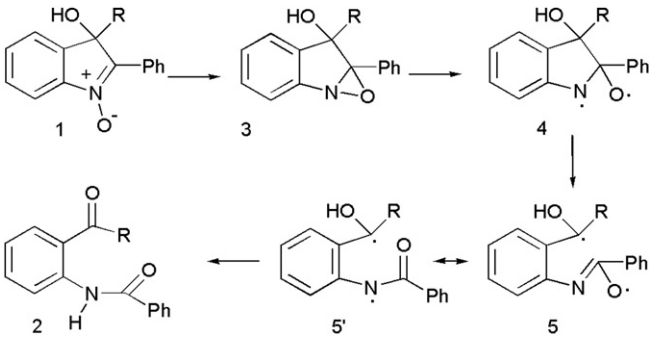

Scheme 2.

In order to verify the radical nature of the photorearrangement of nitrones by evidencing the formation of the radical intermediates shown in Scheme 2, we repeated the reactions in the presence of a radical scavenger and monitored them by means of the EPR-Spin Trapping technique. In particular, benzene solutions of compounds **1a** and **1d** containing a small amount of the spin trap PBN were irradiated in a flat Suprasil® quartz cell for 5 min using an UV-A lamp. Immediately after irradiation, the cell was inserted in the cavity of an EPR spectrometer and spectra were recorded. For both compounds, the recorded spectra (see Fig. 2) resulted from the overlapping of the signals from three different species, their spectral parameters (see Table 1) being fairly similar for the two compounds and only slightly dependent on the nature of the substituent R in position 3 of the indolinic derivatives. Irradiation of compounds **1a** and **1d** in acetonitrile solution, i.e., the same solvent used in the macroscale reactions, also led to the EPR detection of the same spin adducts, with slight variations of their spectral parameters due to the higher solvent polarity (data not shown).

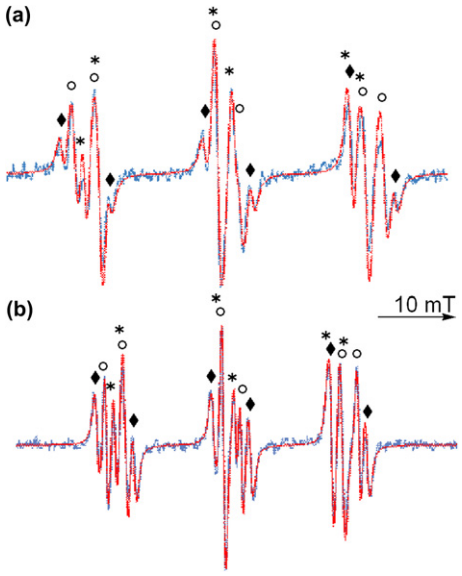

Fig. 2. Room temperature experimental (blue) and computer simulated (red) EPR spectra observed following a 5 min UV-A irradiation of deoxygenated benzene solutions of (a): **1a** and (b): **1d** (○, **6a**,**d**; ✱, **7a**, **d**; ◆, **8a**, **d**).

Table 1
EPR *hfsc* and *g*-factors for the radicals observed after UV-A irradiation of benzene solutions of compounds **1a** and **1d**. DFT computed values in parenthesis

Radical	a_H/mT	a_N/mT	*g*	Amount %
6a	0.221 (0.132)	1.440 (1.403)	2.0057_8 (2.0057_5)	~58
6d	0.215	1.442	2.0058_1	~34
7a	0.150 (0.118)	1.333 (1.304)	2.0060_4 (2.0060_4)	~39
7d	0.143	1.334	2.0060_1	~30
8a	0.456 (0.409)	1.427 (1.376)	2.0058_1 (2.0059_1)	~3
8d	0.452	1.424	2.0058_0	~36

The spectral parameters of the three radical species detected following UV-A irradiation of solutions of **1a** or **1d** in the presence of PBN are in line with nitroxides with a β-alkoxy or a γ-hydroxy substituent,[18–20] resulting from the PBN trapping of whatever radicals may be formed from **1a**,**d**. We then identified the radicals responsible for the observed spectra as nitroxides **6a**,**d**, **7a**,**d**, and **8a**,**d** (Block 1). DFT calculations employing an already published[21] multistep procedure were performed to corroborate our hypotheses. Indeed, as shown in Table 1, a fairly good agreement between experimental and computed data was found concerning both EPR hyperfine splitting constants (*hsfc*) and *g*-factors.

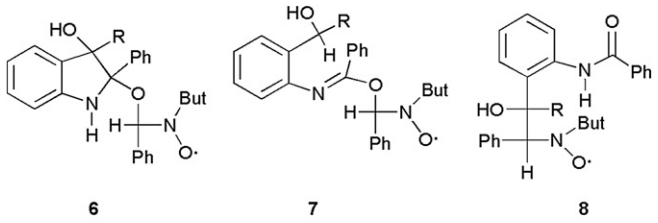

Block 1.

Nitroxides **6**–**8** can be considered as deriving from the interaction of the trap PBN with biradicals **4** and **5**/**5′**, respectively, followed by hydrogen abstraction, and their identity provides support for the mechanism outlined in Scheme 2.

In order to verify the feasibility of the mechanism as proposed in Scheme 2, a thermochemical study was carried out by means of DFT calculations (details in the Experimental section) in which the geometry of each intermediate taken into account corresponds to the conformer lowest in energy among the possible ones, obtained by means of appropriate relaxed Potential Energy Surface (PES) Scans. In Scheme 3, the computed structure of **3a**, **5′a**, and **2a** have been reported in a tube-style representation along with the computed Gibbs Free Energy changes (ΔG^0_{298} in kcal/mol) for each step.

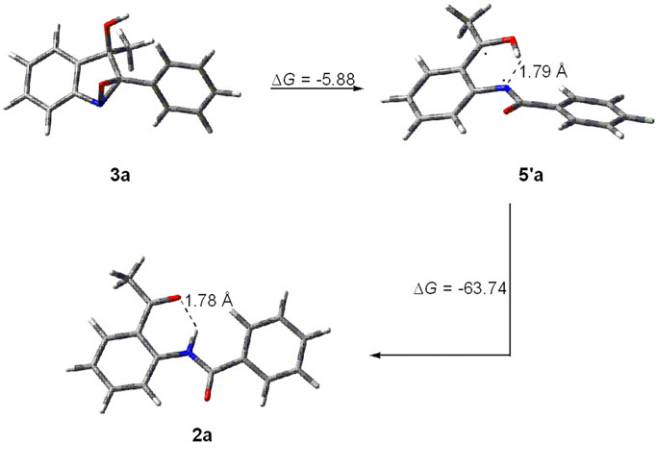

Scheme 3.

As indicated by the Δ*G* values shown in Scheme 3, the first step of the process, i.e., the opening of the oxaziridine ring and the consequent formation of biradical **5**/**5′**, experimentally supported by the detection of nitroxide **8** in the spin trapping experiments, is almost thermoneutral, the overall process being 'driven' by the hydrogen shift leading to the final product. Taking into account the OH–N and the O–HN distances in **5′** and **2** also reported in the scheme, the possibility of a hydrogen bond, with formation of six-membered rings, in both the intermediate **5′** and the final product **2**, seems relevant.

An additional confirmation to our hypothesis came from the results obtained in the photorearrangement of compound **9** (Scheme 4). Indeed **9**, obtained via methylation of the 3-OH group in **1e**, gave upon irradiation benzoxazine **10**, easily identified from its ^{1}H NMR spectrum characterized by two doublets at 8.23 and 8.27 ppm (*J*=1.62 Hz) typical of the *ortho* protons in the C-2 phenyl ring of the N=C–Ph moiety.

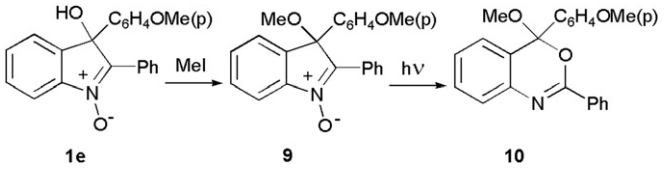

Scheme 4.

In fact, benzoxazine **10** could derive from a radical intermediate analogous to **5**/**5′** shown in Scheme 2: since in this case no hydrogen transfer is possible due to the methylation of the OH group, an intramolecular coupling may lead to the isolated product **10**.

Even if spin trapping experiments do support the participation of radical intermediates in the photorearrangement of nitrones, other mechanisms not involving the participation of radical species may not be excluded. In this context it should be borne in mind that EPR spectroscopy is a very sensitive technique (radical concentration $\geq 10^{-7}$ M) and that the detection of free radicals in the course of a reaction does not necessarily mean that they are the only possible intermediates or even lie on the main reaction coordinate.

For this reason, DFT calculations were carried out by imposing a singlet state for each intermediate (**11** and **12**, Block 2) and in Scheme 5 a mechanism, chosen among the possible pathways, is shown together along with the computedΔG^0_{298} (in kcal/mol) for each step.

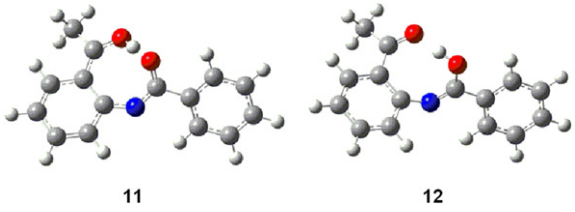

Block 2.

Contrary to the radical mechanism previously proposed, in this case the most exergonic process is now the first step, i.e., the formation of **11**, which would rearrange to give the final reaction product through isomer **12**. The O–HO distances in **11** and **12** are 1.43 and 1.78 Å, respectively, and also in this case the possibility of hydrogen bonding could play an important role, although with the formation of eight-membered rings.

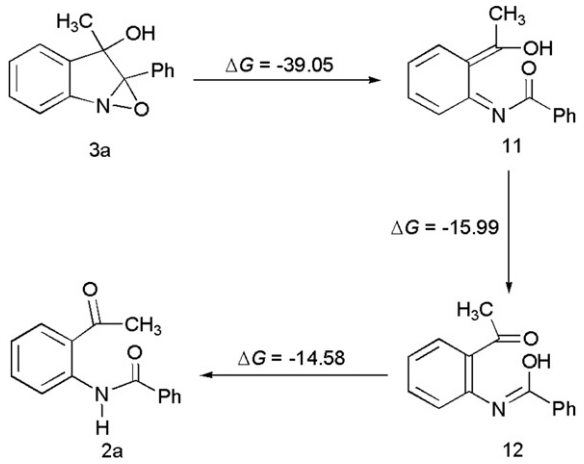

Scheme 5.

3. Conclusion

The ring-opening photoisomerization of the title compounds **1** to *N*-(acylphenyl)benzamides **2** is logically explained by initial conversion of **1** into the corresponding indolooxaziridines **3**. N–O bond homolysis of the latter with concomitant homolytic indole C2–C3 bond breakage, followed by hydrogen migration (from OH to N), is regarded feasible on the basis of DFT calculations. In addition, spin trapping experiments serve well as direct experimental support of the (at least in part) homolytic character of the ring-opening reactions of the oxaziridine intermediates.

4. Experimental

4.1. Chemicals

PBN, methylmagnesium chloride, *i*-propylmagnesium chloride, *n*-butylmagnesium chloride, phenylmagnesium bromide, *p*-methoxyphenylmagnesium bromide, benzylmagnesium chloride, methyl iodide, and potassium hydroxide were purchased from Aldrich. Benzene, acetonitrile, and dimethyl sulfoxide were of pure grade and used without any further purification. 2-Phenylisatogen was prepared as reported in the literature.[22]

4.2. Calculations

Density Functional Theory[23] calculations were carried out using the GAUSSIAN 09 suite of programs[24] on an IBM SP-6 at Cineca Supercomputing Center.[25] All calculations on paramagnetic species were carried out with the unrestricted formalism, giving $<S^2>=0.7501\pm0.0003$ for spin contamination (after annihilation), and performed following the multistep procedure previously described.[21] In addition, in frequency calculations, imaginary (negative) values were never found, confirming that the computed geometries were always referred to a minimum. Isotropic *g*-factors was determined by means of the Gauge Independent Atomic Orbital method[26] as the average of the *xx*, *yy*, and *zz* corresponding components. It should be noted that all radicals and all closed-shell species considered in this study were true minimum energy structures (i.e., having no imaginary frequencies). All geometries were optimized at the B3-LYP/6-31G(d) level of theory, with conformations systematically screened by means of appropriate relaxed (i.e., with optimization at each point) Potential Energy Surface Scans to ensure that species were global minimum energy structures. Thermodynamic quantities have been computed at 298 K by means of frequency calculations performed employing the M06-2X[27] functional in conjunction with the 6-31+G(d,p) basis set.

4.3. Instrumentation

Melting points are uncorrected and were measured with an Electrothermal apparatus. ^{13}C and ^{1}H NMR spectra were recorded at room temperature in $CDCl_3$ or DMSO-d_6 solution on a Varian 400 spectrometer using TMS as reference; *J* values are given in hertz. IR spectra were recorded in the solid state with a Perkin–Elmer MGX1 spectrophotometer equipped with Spectra Tech. Mass spectra and exact mass measurements were performed with a Finnigan Mat95XP spectrometer in EI ionization mode. EPR spectra were run with a Bruker EMX EPR spectrometer equipped with an NMR Gauss meter for field calibration and an XL Model 3120 microwave frequency counter meter for *g*-factor determination. Typical instrumental settings were: modulation frequency 100 kHz, modulation amplitude 0.04 mT, sweep width 4.0 mT, microwave power 5 mW, time constant 1.28 s, receiver gain 5×10^3.

Irradiation was carried out using a Philips Original Home Solarium, model HB 406/A equipped with a Philips HPA/400 W lamp, whose irradiance in the range 300–400 nm was 0.75 mW/cm^2.

4.4. EPR measurements

Nitrones **1a** and **1d** (4 mg in 0.5 mL of benzene) and PBN (4 mg in 0.5 mL of benzene) were put separately into the two arms of an inverted U tube equipped with a flat quartz cell.[29] The thoroughly nitrogen purged solutions were mixed, transferred into the aqueous flat cell and irradiated for 5 min maintaining the cell at 30 cm from the UV-A lamp. The cell was then put into the EPR cavity and the signal recorded.

Computer simulation of EPR spectra was achieved using the WinSim program in the NIEHS public ESR software tools package (www.epr.niehs.nih.gov),[30] or a program based on a Montecarlo minimization procedure.[31]

4.5. Synthesis of nitrones 1a–f

Nitrones **1a–f** were synthesized according to a literature procedure:[28] the appropriate Grignard reagent (10 mmol) was added dropwise to a solution of 2-phenylisatogen (5 mmol, 1.12 g in 80 mL of anhydrous THF), under stirring and in a current of nitrogen. After 2 h the reaction mixture was poured into 10% aqueous NH_4Cl (100 mL) and extracted with diethyl ether. The organic layer, dried over Na_2SO_4, was evaporated to dryness and the residue was washed with diethyl ether/hexane 80:20. The insoluble product was the expected nitrone, which was separated by filtration under vacuum.

4.5.1. 3-Hydroxy-3-methyl-2-phenyl-3H-indole N-oxide ***1a***. Yield 70%. Mp 246–247 °C from acetic acid/ligroin 80–100 °C; FT-IR, ν, cm^{-1} 3152, 1450, 764; δ_H (400 MHz DMSO-d_6) 1.67 (3H, s, Me), 6.44 (1H, br s, OH), 7.50–7.58 (5H, m, arom), 7.67–7.69 (2H, m, arom), 8.84–8.86 (2H,m, arom); δ_C (100.49 MHz DMSO-d_6) 145.0, 145.0, 139.8, 130.0, 129.6, 129.4, 128.3, 128.0, 127.4, 121.9, 114.2, 78.0, 25.6; *m*/*z* 239 (23, M$^+$), 207 (17.5), 196 (53.4), 105 (89.3), 77 (84.2). HRMS (EI) *m*/*z* calcd for $C_{15}H_{13}NO_2$ (M$^+$): 239.0946; found 239.0949.

4.5.2. 3-Hydroxy-2-phenyl-3-(2-propyl)-3H-indole N-oxide ***1b***. Yield 73%. Mp 224–225 °C from acetone/ligroin 80–100 °C; FT-IR, ν, cm^{-1} 3150, 1465, 763; δ_H (400 MHz, $CDCl_3$) 0.07 (3H, d, Me, *J* 7.0 Hz), 1.25 (3H, d, Me, *J* 7.0 Hz), 2.35–2.45 (1H, septet, CH, *J* 7.0 Hz), 5.89 (1H, br s, OH), 6.91–6.95 (1H, m, arom), 7.08 (1H, d, arom, *J* 7.8 Hz), 7.15 (1H,

p-triplet, arom), 7.19–7.28 (3H, m, arom), 7.45 (1H, d, arom, *J* 7.0 Hz), 8.48 (2H, d, arom, *J* 7.8 Hz); δ_C (100.49 MHz, $CDCl_3$) 144.8, 135.0, 130.6, 129.4, 128.5, 127.8, 127.1, 123.4, 114.2, 84.8, 35.8, 16.4, 15.8; *m*/*z* 267 (M^+, 6.5), 223 (100), 207 (20.7), 179 (60.05), 105 (56.9), 77 (55.8). HRMS (EI) *m*/*z* calcd for $C_{17}H_{17}NO_2$ (M^+): 267.1259; found 239.1255.

4.5.3. 3-n-Butyl-3-hydroxy-2-phenyl-3H-indole N-oxide ***1c***. Yield 68%. Mp 155–156 °C from acetone/ligroin 80–100 °C; FT-IR, *ν*, cm^{-1} 3110, 1461, 755; δ_H (400 MHz, $CDCl_3$) 0.28–0.5 (2H, m, CH_2), 0.51 (3H, t, Me, *J* 7.0 Hz), 0.88–0.97 (2H, m, CH_2), 2.01–2.18 (2H, m, CH_2), 6.19(1H, br s, OH), 6.83 (1H, t, arom, *J* 7.8 Hz), 7.01 (1H, d, arom, *J* 7.8 Hz), 7.15 (1H, t, arom, *J* 7.8 Hz), 7.21–7.31 (3H, m, arom), 7.41 (1H, d, arom, *J* 7.0 Hz), 8.48 (2H, d, arom, *J* 7.0 Hz); δ_C (100.49 MHz, $CDCl_3$) 147.9, 144.2, 137.4, 130.6, 129.2, 128.9, 128.3, 127.9, 127.0, 121.5, 119.5, 114.2, 81.8, 38.4, 24.7, 22.3, 13.5; *m*/*z* 281 (M^+,5.0), 265 (11.3), 236 (41.5), 208 (100), 193 (17.4), 180 (12.8), 77 (17.3); HRMS (EI) *m*/*z* calcd for $C_{18}H_{19}NO_2$ (M^+): 281.1416; found 281.1417.

4.5.4. 3-Hydroxy-2,3-diphenyl-3H-indole N-oxide ***1d***. Yield 80%. Mp 250–251 °C from acetic acid; FT-IR, *ν*, cm^{-1} 3159, 1445, 758; δ_H (400 MHz DMSO-d_6) 7.15 (1H, s, OH), 7.20–7.23 (1H, *m*, arom), 7.28–7.31 (3H, m, arom), 7.34–7.45 (6H, m, arom), 7.53 (1H, t, arom, *J* 7.8 Hz), 7.74 (1H, d, arom, *J* 7.8 Hz), 8.56–8.59 (2H, m, arom); δ_C (100.49 MHz DMSO-d_6) 146.0, 145.8, 141.9, 140.9, 130.6, 130.5, 130.1, 129.4, 128.7, 128.2, 128.1, 125.0, 123.4, 115.1, 82.0; *m*/*z* 301 (M^+, 27.3), 281 (25.7), 207 (66.3), 196 (48.7), 105 (100), 77 (71.2); HRMS (EI) *m*/*z* calcd for $C_{20}H_{15}NO_2$ (M^+): 301.1103; found 301.1104.

4.5.5. 3-Hydroxy-3-(p-methoxyphenyl)-2-phenyl-3H-indole N-oxide ***1e***. Yield 75%. Mp 240 °C from acetic acid; FT-IR, *ν*, cm^{-1} 3081, 1443, 752; δ_H (400 MHz DMSO-d_6) 3.7 (3H, s, OMe), 6.85 (2H, d, arom, *J* 8.6 Hz), 7.1 (1H, s, OH), 7.25–7.28 (3H, m, arom), 7.39–7.43 (4H, m, arom), 7.53 (1H, t, arom, *J* 7.8 Hz), 7.73 (1H, d, arom, *J* 8.0 Hz), 8.59–8.61 (2H, m, arom); δ_C (100.49 MHz DMSO-d_6) 159.0, 145.7, 145.5, 141.0, 133.4, 130.4, 130.3, 129.8, 128.5, 128.1, 128.1, 126.2, 123.1, 114.8, 114.6, 81.6, 55.5; *m*/*z* 331 (M^+, 22.6), 226 (25.2), 207 (20.4), 196 (45.1), 135 (11.4), 105 (100), 77 (78.8); HRMS (EI) *m*/*z* calcd for $C_{21}H_{17}NO_3$ (M^+): 331.1208; found 331.1206.

4.5.6. 2-Phenyl-3-benzyl-3-hydroxy-3H-indole N-oxide ***1f***. Yield 72%; Mp 205–206 °C from aceton/petrolether; FT-IR, *ν*, cm^{-1} 3214, 1445, 763; δ_H (400 MHz, $CDCl_3$) 3.28 (2H, quartet, CH_2Ph, *J* 13.32 Hz), 6.04 (1H, br s, OH), 6.21 (2H, d, arom, *J* 8.6 Hz), 6.64–6.72 (4H, m, arom), 6.80–6.83 (1H, m, arom), 6.94–6.98 (1H, m, arom), 7.08–7.22 (4H, m, arom), 8.38 (2H, d, arom, *J*=8.6 Hz); δ_C (100.49 MHz, $CDCl_3$) 136.5, 133.7, 130.6, 129.8, 129.4, 128.5, 128.1, 127.6, 127.5, 126.7, 122.4, 119.2, 114.0, 82.1, 44.4; *m*/*z* 315 (M^+, 20.6), 286 (100), 242(20.5), 207 (15.8), 105 (6.2), 77 (21.3); HRMS (EI) *m*/*z* calcd for $C_{21}H_{17}NO_2$ (M^+): 315.1259; found 315.1257.

4.6. Irradiation of 1a–f. General procedure

The nitrone (0.33 mmol) was dissolved in 50 mL of dried acetonitrile and put into a quartz tube. The solution was purged with argon and then irradiated with an UV-A lamp under magnetic stirring at 30 cm distance from the lamp. After 20 min, the starting material was completely consumed as evidenced by TLC (thin layer chromatography) and eluted with cyclohexane/ethylacetate 8:2. Only the corresponding rearranged compound was quantitatively recovered, demonstrating the complete transformation of the nitrone. After the evaporation of the solvent, the residue was purified by crystallization from toluene/petroleum ether. *N*-(2-Acetylphenyl)benzamide **2a** and *N*-(2-benzoylphenyl)benzamide **2d** were identified by comparison with authentic samples commercially available.

4.6.1. N-[2-(2-Methylpropanoyl)phenyl]benzamide ***2b***. Mp 106–107 °C; FT-IR, *ν*, cm^{-1} 3210, 1673, 1586; δ_H (400 MHz, $CDCl_3$) 1.26 (6H, d, 2×Me, *J* 7.0 Hz), 3.71 (1H, septet, *J* 7.0 Hz), 7.17 (1H, t, arom, *J* 7.0 Hz),7.51–7.57 (3H, m, arom), 7.62 (1H, t, arom, *J* 8.6 Hz), 8.03 (1H, d, arom, *J* 8.6 Hz), 8.07 (2H, dd, arom, *J* 7.8 and 1.6 Hz), 8.97 (1H, d, arom, *J* 8.6 Hz), 12.71 (1H, br, NH); δ_C (100.49 MHz, $CDCl_3$) 209.5, 166.1, 141.8, 134.9, 131.9, 130.7, 128.8, 127.5, 122.5, 121.3, 121.0, 36.3, 15.6; *m*/*z* 267 (M^+, 2.6), 224 (100), 196 (4.3), 146 (12.8), 105 (67.6), 77 (61.1); HRMS (EI) *m*/*z* calcd for $C_{17}H_{17}NO_2$ (M^+): 267.1259; found 267.1258.

4.6.2. N-(2-Butanoylphenyl)benzamide ***2c***. Mp 70–71 °C; FT-IR, *ν*, cm^{-1} 3208, 1673, 1585; δ_H (400 MHz, $CDCl_3$) 0.98 (3H, t, Me, *J* 7.8 Hz), 1.41–1.47 (2H, m, CH_2), 1.72–1.77 (2H, m, CH_2), 3.07 (2H, t, CH_2, *J* 7.8 Hz), 7.16 (1H, t, arom, *J* 7.0 Hz), 7.52–7.64 (4H, m, arom), 7.98 (1H, d, arom, *J* 8.0 Hz), 8.08 (2H, d, arom, *J* 6.2 Hz), 8.98 (1H, d, arom, *J* 7.8 Hz), 12.37 (1H, br, NH); δ_C (100.49 MHz, $CDCl_3$) 205.6, 166.1, 141.4, 135.0, 131.9, 130.9, 128.8, 127.5, 122.4, 121.9, 121.0, 39.9, 27.0, 22.4, 13.9; *m*/*z* 281 (M^+, 7.2), 224 (80.7), 196 (23.1), 146 (7.1), 105 (100), 77 (71.9); HRMS (EI) *m*/*z* calcd for $C_{18}H_{19}NO_2$ (M^+): 281.1416; found 281.1417.

4.6.3. N-[2-(p-Methoxybenzoyl)phenyl]benzamide ***2e***. Mp 113–114 °C; FT-IR, *ν*, cm^{-1} 3229, 1672, 1624, 1583; δ_H (400 MHz, $CDCl_3$) 3.89 (3H, s, OMe), 6.98 (2H, d, arom, *J* 8.6 Hz), 7.14 (1H, *p*-triplet, arom), 7.49–7.55 (3H, m, arom), 7.61–7.64 (2H, m, arom), 7.76 (2H, d, arom, *J* 8.6 Hz), 8.04 (2H, dd, arom, *J* 1.6 and 7.9 Hz), 8.83 (1H, d, arom, *J* 7.8 Hz), 11.70 (1H, br, NH); δ_C (100.49 MHz, $CDCl_3$) *198.5*, *165.7*, *163.3*, *140.5*, *134.6*, *133.9*, *133.3*, *132.6*, *131.9*, *131.1*, *128.8*, *127.4*, *124.1*, *122.1*, *121.6*, *113.6*, *55.5*; *m*/*z* 331 (M^+, 21.5), 226 (18.2), 196 (53.5), 135 (9.5), 105 (100), 77 (67); HRMS (EI) *m*/*z* calcd for $C_{21}H_{17}NO_3$ (M^+): 331.1208; found 331.1206.

4.6.4. N-(2-Phenylacetyl)phenylbenzamide ***2f***. Mp 142–143 °C; FT-IR, *ν*, cm^{-1} 3220, 1675,, 1587; δ_H (400 MHz, $CDCl_3$) 4.38 (2H, s, CH_2Ph), 7.16 (1H, t, arom, *J* 7.0 Hz), 7.27–7.30 (3H, m, arom), 7.34–7.38 (2H, m, arom), 7.48–7.55 (3H, m, arom), 7.62 (1H, t, arom, *J* 8.6 Hz), 8.05 (2H, d, arom, *J* 6.3 Hz), 8.1 (1H, d, arom, *J* 7.8 Hz), 8.99 (1H, d, arom, *J* 8.6 Hz), 12.6 (1H, br, NH); δ_C (100.49 MHz, $CDCl_3$) *202.5*, *166.2*, *135.4*, *134.7*, *134.3*, *131.9*, *131.5*, *129.4*, *128.8*, *128.8*, *127.5*, *127.1*, *122.5*, *121.1*, *46.9*; *m*/*z* 315 (M^+, 0.8), 224 (100), 146 (15.5), 105 (57), 22 (52.7); HRMS (EI) *m*/*z* calcd for $C_{21}H_{17}NO_2$ (M^+): 315.1259; found 315.1256.

4.7. Synthesis of compound 9

To a suspension of potassium hydroxide (1.12 g, 20 mmol) in dimethyl sulfoxide (20 mL), nitrone **1e** (1.65 g, 5 mmol) and methyl iodide (1.06 g, 7.5 mmol) were added and the reaction mixture was stirred at room temperature for 30 min. Water (20 mL) was then added to the reaction mixture that was afterward extracted with methylene chloride (20 mL). The organic layer was repeatedly washed with water (5–10 times), dried over anhydrous Na_2SO_4 and the solvent was removed under reduced pressure.

4.7.1. 3-Methoxy-3-(p-methoxyphenyl)-2-phenyl-3H-indole N-oxide ***9***. FT-IR, *ν*, cm^{-1} 1607, 1510, 1441, 794; δ_H (400 MHz, $CDCl_3$) 3.06 (3H, s, $-OCH_3$), 3.73 (3H, s, Ph$-OCH_3$), 6.78 (2H, d, arom, *J* 9.4 Hz), 7.24 (1H, d, *J* 7.0 Hz), 7.32 (2H, d, *J* 8.6 Hz), 7.37–7.39 (5H, m, arom), 7.51 (1H, t, arom, *J* 7.8 Hz), 7.89 (1H, d, arom, *J* 7.8 Hz), 8.64–8.67 (2H, m, arom,); δ_C (100.49 MHz, $CDCl_3$) 159.2, 136.0, 131.9, 130.5, 128.3, 127.7, 126.1, 122.8, 115.0, 114.1, 87.9, 55.1, 52.1; *m*/*z* 345 (M^+, 21.5),

314 (24.7), 240 (100), 210 (27.8), 135(22.0), 105 (63.5), 77 (45.5); HRMS (EI) *m*/*z* calcd for $C_{22}H_{19}NO_3$ (M^+): 345.1365; found 345.1363.

4.8. Irradiation of compound 9

Nitrone **9** (114 mg, 0.33 mmol) was dissolved in 50 mL of acetonitrile in a quartz tube. The solution was purged with argon and then irradiated with the UV-A lamp under magnetic stirring at 30 cm distance. After 20 min a TLC (cyclohexane/ethylacetate 8:2) showed the complete transformation of the starting material and the only spot observed was that corresponding to the rearranged compound, indicating the quantitative transformation of the nitrone. Evaporation of the solvent gave a solid residue, which was submitted to spectroscopic analysis.

*4.8.1. 4-Methoxy-4-(p-methoxyphenyl)-2-phenyl-4H-benzo[1,3]oxazine **10**.* FT-IR, ν, cm^{-1} 1599, 1511, 1253, 764; δ_H (400 MHz, $CDCl_3$) 3.30 (3H, s, $-OCH_3$), 3.82 (3H, s, Ph$-OCH_3$), 6.82 (2H, d, arom, *J* 8.6 Hz), 7.02–7.06 (1H, m, arom), 7.14–7.21 (1H, m, arom), 7.34–7.51 (7H, m, arom), 8.24 (2H, d, arom, *J* 8.6 Hz); δ_C (100.49 MHz, $CDCl_3$) 159.8, 155.6, 140.0, 133.6, 131.4, 129.8, 128.4, 128.1, 127.9.126.7, 126.3, 125.4, 124.5, 113.5, 103.2, 55.3, 51.1; *m*/*z* 345 (M^+, 39.4), 330 (14.6), 329 (41.0), 314 (100), 286 (35.8), 195 (15.5), 135 (53.9), 105 (26.7); HRMS (EI) *m*/*z* calcd for $C_{22}H_{19}NO_3$ (M^+): 345.1365; found 345.1362.

4.9. Single crystal X-ray analysis of compound 2d

Crystallographic data were collected at room temperature on a Siemens AED diffractometer using Cu Kα radiation (λ=1.54178 Å). Data were corrected for Lorentz and polarization effects but not for absorption. The structures were solved by direct methods (SIR97)[32] and anisotropically refined for all the non-H atoms. The refinements were performed on F^2 using SHELXL-97.[33] All H atoms were placed at calculated positions and refined using a riding model approximation, with C–H=0.93–0.96 Å, N–H=0.86 Å, and with U_{iso}(H)=1.2 U_{eq}(C, N). $C_{20}H_{15}NO_2$, M_r=301.33, triclinic, space group *P*–1, *a*=7.201 (2), *b*=8.417 (2), *c*=13.159 (3) Å, α=90.793 (3), β=100.486 (3), γ=93.182 (3)°, *V*=782.8 (3) $Å^3$, *Z*=2, ρ_{calc}=1.278 g cm^{-3}, μ=0.661 mm^{-1}; yellow block, crystal dimensions 0.18×0.23×0.28 mm, 212 parameters, *R*=0.048, wR_2=0.113 (for 2973 unique reflections, $I>0$), *S*=0.993, $\Delta\rho$ (min/max)=–0.12/0.15 e $Å^{-3}$. Crystallographic data for this structure have been deposited with the Cambridge Crystallographic Data Center as supplementary publication number CCDC 815157.

Acknowledgements

P.C. and P.S. would like to thank MIUR (Ministero dell'Università e della Ricerca Scientifica e Tecnologica) for financial support (PRIN 2008); P.S. is grateful to Cineca Supercomputing Center for computational resource allocation (ISCRA grant NMPNITRO, code: HP10CAQFF04).

Supplementary data

Supplementary data associated with this article can be found in the online version at doi:10.1016/j.tet.2011.06.094.

References and notes

1. Spence, G. G.; Taylor, E. C.; Buchardt, O. *Chem. Rev.* **1970**, *70*, 231–265.
2. Padwa, A. *Chem. Rev.* **1977**, *77*, 37–68.
3. Albini, A.; Alpegiani, M. *Chem. Rev.* **1984**, *84*, 43–71.
4. Eckroth, D. R.; Squire, R. H. *J. Org. Chem.* **1971**, *36*, 224–226.
5. Albini, A.; Fasani, E.; Buchardt, O. *Tetrahedron Lett.* **1982**, *23*, 4849–4852.
6. Albini, A.; Fasani, E.; Maggi Decrema, L. *J. Chem. Soc., Perkin Trans. 1* **1980**, 2738–2742.
7. Albini, A.; Fasani, E.; Frattini, V. *J. Chem. Soc., Perkin Trans. 2* **1988**, 235–240.
8. Kondo, H.; Tanaka, K.; Kubo, K.; Igarashi, T.; Sakurai, T. *Heterocycles* **2004**, *63*, 241–247.
9. Zeng, Y.; Smith, B. T.; Hershberger, J.; Aubé, J. *J. Org. Chem.* **2003**, *68*, 8065–8067.
10. Bourguet, E.; Baneres, J.-L.; Girard, J.-P.; Parello, J.; Vidal, J.-P.; Lusinchi, X.; Declercq, J.-P. *Org. Lett.* **2001**, *3*, 3067–3070.
11. Ogata, M.; Matsumoto, H.; Takahashi, S.; Kanō, H. *Chem. Pharm. Bull.* **1970**, *18*, 964–969.
12. Oliveros, E.; Rivière, M.; Lattes, A. *J. Heterocycl. Chem.* **1980**, *17*, 1025–1027.
13. Colonna, M.; Poloni, M. *Ann. Chim. (Rome, Italy)* **1973**, *63*, 287–289.
14. Usman, A.; Razak, I. A.; Fun, H.-K.; Chantrapromma, S.; Tian, J.-Z.; Zhang, Y.; Xu, J.-H. *Acta Crystallogr.* **2002**, *E58*, o492–o494.
15. Döpp, D.; Weiler, H. *Tetrahedron Lett.* **1974**, *15*, 2445–2448.
16. Döpp, D. *Chem. Ber.* **1976**, *106*, 3849–3863.
17. Döpp, D. *Tetrahedron Lett.* **1972**, *13*, 3215–3218.
18. Forrester, A. R. In *Landolt-Börnstein—Magnetic Properties of Free Radicals*; Fischer, H., Hellwege, K.-H., Eds.; Springer: Heidelberg, 1979; II/9c1.
19. Forrester, A. R. In *Landolt-Börnstein—Magnetic Properties of Free Radicals*; Fischer, H., Ed.; Springer: Heidelberg, 1989; II/17d2.
20. Alberti, A. In *Landolt-Börnstein—Magnetic Properties of Free Radicals*; Fischer, H., Ed.; Springer: Heidelberg, 2005; II/26d.
21. Stipa, P. *Chem. Phys.* **2006**, *323*, 501–510.
22. Bond, C. C.; Hooper, M. *Synthesis* **1974**, *6*, 443.
23. (a) *Density Functional Theory of Atoms and Molecules*; Parr, R. G., Yang, W., Eds.; Oxford University: New York, NY, 1998; (b) *A Chemists Guide to Density Functional Theory*; Koch, W., Holthausen, M. C., Eds.; Wiley-VCH: Weinheim, 2000.
24. Frisch, M. J.; Trucks, G. W.; Schlegel, H. B.; Scuseria, G. E.; Robb, M. A.; Cheeseman, J. R.; Montgomery, J. A., Jr.; Vreven, T.; Kudin, K. N.; Burant, J. C.; Millam, J. M.; Iyengar, S. S.; Tomasi, J.; Barone, V.; Mennucci, B.; Cossi, M.; Scalmani, G.; Rega, N.; Petersson, G. A.; Nakatsuji, H.; Hada, M.; Ehara, M.; Toyota, K.; Fukuda, R.; Hasegawa, J.; Ishida, M.; Nakajima, T.; Honda, Y.; Kitao, O.; Nakai, H.; Klene, M.; Li, X.; Knox, J. E.; Hratchian, H. P.; Cross, J. B.; Bakken, V.; Adamo, C.; Jaramillo, J.; Gomperts, R.; Stratmann, R. E.; Yazyev, O.; Austin, A. J.; Cammi, R.; Pomelli, C.; Ochterski, J. W.; Ayala, P. Y.; Morokuma, K.; Voth, G. A.; Salvador, P.; Dannenberg, J. J.; Zakrzewski, V. G.; Dapprich, S.; Daniels, A. D.; Strain, M. C.; Farkas, O.; Malick, D. K.; Rabuck, A. D.; Raghavachari, K.; Foresman, J. B.; Ortiz, J. V.; Cui, Q.; Baboul, A. G.; Clifford, S.; Cioslowski, J.; Stefanov, B. B.; Liu, G.; Liashenko, A.; Piskorz, P.; Komaromi, I.; Martin, R. L.; Fox, D. J.; Keith, T.; Al-Laham, M. A.; Peng, C. Y.; Nanayakkara, C. Y. A.; Challacombe, M.; Gill, P. M. W.; Johnson, B.; Chen, W.; Wong, M. W.; Gonzalez, C.; Pople, J. A. *Gaussian 09, Revision B.01*; Gaussian: Wallingford, CT, 2010.
25. Cineca Supercomputing Center (via Magnanelli 6/3, I-40033 Casalecchio di Reno, Italy; http://www.cineca.it/HPSystems).
26. (a) London, F. *J. Phys. Radium* **1937**, 397–409; (b) McWeeny, R. *Physiol. Rev.* **1962**, *126*, 1028–1034; (c) Ditchfield, R. *Mol. Phys.* **1974**, *27*, 789–807; (d) Cheeseman, J. R.; Trucks, G. W.; Keith, T. A.; Frisch, M. J. *J. Chem. Phys.* **1996**, *104*, 5497–5509; (e) Wolinski, K.; Hinton, J. F.; Pulay, P. *J. Am. Chem. Soc.* **1990**, *112*, 8251–8261.
27. Zhao, Y.; Truhlar, D. G. *Theor. Chem. Acc.* **2008**, *120*, 215–241.
28. Berti, C.; Colonna, M.; Greci, L.; Marchetti, L. *Tetrahedron* **1975**, *31*, 1745–1753.
29. Russell, G. A.; Janzen, E. G.; Strom, E. T. *J. Am. Chem. Soc.* **1964**, *86*, 1807–1814.
30. Duling, D. R. *J. Magn. Reson., Ser. B* **1994**, *104*, 105–110.
31. Lucarini, M.; Luppi, B.; Pedulli, G. F.; Roberts, B. P. *Chem.—Eur. J.* **1999**, *5*, 2048–2054.
32. Altomare, A.; Burla, M. C.; Camalli, M.; Cascarano, G.; Giacovazzo, C.; Guagliardi, A.; Moliterni, A. G. G.; Polidori, G.; Spagna, R. *J. Appl. Crystallogr.* **1999**, *32*, 115–119.
33. Sheldrick, G. M. *Acta Crystallogr.* **2008**, *A64*, 112–122.